RSC Advances

PAPER

View Article Online
View Journal | View Issue

Cite this: *RSC Adv.*, 2019, **9**, 36058

Synthesis and properties of hyperbranched polymers for white polymer light-emitting diodes†

Xuefeng Li,[ab] Haocheng Zhao,[cd] Long Gao,[b] Xiaoling Xie,*[a] Weixuan Zhang,[ab] Mixue Wang,[b] Yuling Wu,*[b] Yanqin Miao,[b] Hua Wang[b] and Bingshe Xu[b]

Received 13th September 2019
Accepted 29th October 2019

DOI: 10.1039/c9ra07371j

rsc.li/rsc-advances

In this work, a series of hyperbranched copolymers with fluorene-*alt*-carbazole as the branches, three-dimensional-structured spiro[3.3]heptane-2,6-dispirofluorene (SDF) as the core, and iridium 1-(4-bromophenyl)-isoquinoline (acetylacetone) (Ir(Brpiq)$_2$acac) as the dimming group were synthesized by one-pot Suzuki polycondensation for white emission. All copolymers show great thermal stabilities and high hole-transporting ability due to the introduction of the carbazole unit. The hyperbranched structures for copolymers can suppress the interchain interactions efficiently, and help to form amorphous films. The fabricated polymer light-emitting devices (PLEDs) based on the above synthesized copolymers realize good white light emission, and achieve high electroluminescence (EL) performance. For example, for the optimized PLED, the maximum luminance and current efficiency reach 6210 cd m^{-2} and 6.30 cd A^{-1}, respectively, indicating the synthesized hyperbranched copolymers have potential application in solution-processable white polymer light-emitting diodes.

Introduction

Hyperbranched polymers, as a new type of photoelectric material, have attracted more and more attention.[1–6] This kind of material has a three-dimensional molecular structure, which can cause large steric hindrance in the distribution of the polymer chains to restrain the concentration quenching intermolecular interaction. Three-dimensional hyperbranched structures with globular features can impart polymers with specific advantages relative to their linear counterparts, such as enhanced solubility, thermal stability, and luminous efficiency.[4,7–10] Moreover, the hyperbranched polymers can be synthesized by one-step or quasi-one-step methods. Compared with monodisperse dendrimers, the synthesis and purification process for hyperbranched polymers is simpler, and also shows a lower cost in synthesis.[11] Meanwhile, white polymer light-emitting devices (WPLEDs) have gained extensive attention owing to their potential applications in solid lighting sources and large-area full-color displays, and they also exhibit great advantages such as high contrast, high stability, low price and easy fabrication.[12–14] A conventional approach to gain white-light emission is to synthesize single molecule polymers with blue light emitting groups and complementary orange light emitting units or green and red light emitting units.[13,15,16] Therefore, in order to obtain white organic light emitting diodes (OLEDs), we introduce the broad spectral red light-emitting groups into the hyperbranched polymer.[17]

In this paper, we successfully synthesized the white emitting hyperbranched polymers by selecting fluorene-*alt*-carbazole as the branches, three-dimensional-structured spiro[3.3]heptane-2,6-dispirofluorene (SDF) as the core, and the red phosphor group bis(1-phenyl-isoquinoline) (acetylacetonato)iridium(III) (Ir(Brpiq)$_2$acac) as a dimming functional group. It is found the synthesized hyperbranched polymers show a three-dimensional structure with very good morphological stability and strong fluorescence characteristics. And such three-dimensional structure can also effectively inhibit the entanglement of adjacent alkyl chains through its large steric hindrance, reducing the tight packing of molecular chains and the interaction between the various chromophores in the solid state, which is beneficial for achieving high-performance WPLEDs by suppressing the aggregation of the rigid conjugated polyfluorene material and improving the electroluminescence property.[18,19] Further, we fabricates the PLEDs by employing above synthesized copolymers as light-emitting layer. As we expected that all resulting PLEDs realize good white light emission, and achieve high electroluminescence (EL) performance. For example, for the optimized PLED, the maximum luminance and current efficiency reach 6210 cd m^{-2} and 6.30 cd A^{-1}, respectively.

[a]*College of Materials Science and Engineering, Taiyuan University of Technology, Taiyuan 030024, China. E-mail: xiexiaoling@tyut.edu.cn*

[b]*Key Laboratory of Interface Science and Engineering in Advanced Materials, Taiyuan University of Technology, Taiyuan, 030024, China. E-mail: wuyuling@tyut.edu.cn*

[c]*Department of Electrical Engineering, Shanxi Institute of Energy, Taiyuan 030600, China*

[d]*College of Materials Science and Engineering, Taiyuan University of Science and Technology, Taiyuan 030024, China*

† Electronic supplementary information (ESI) available: ^{1}H NMR and ^{13}C NMR characterization of the complexes and hyperbranched polymers, the PL spectra of green and red phosphor groups. See DOI: 10.1039/c9ra07371j

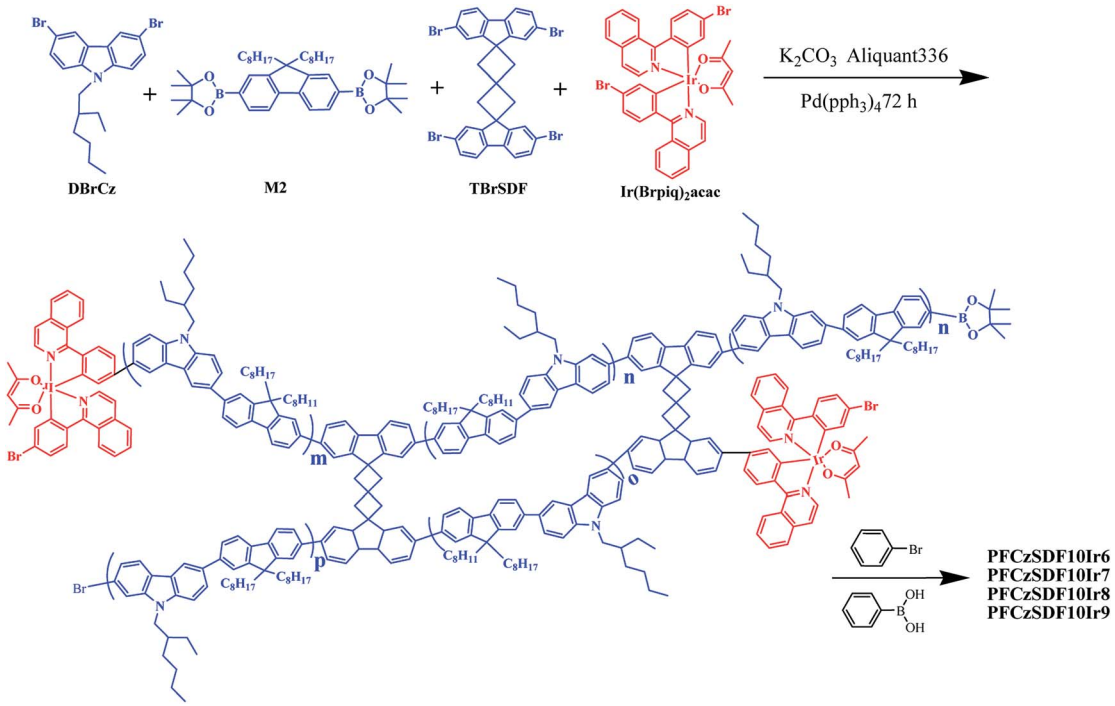

Scheme 1 Synthesis of the hyperbranched copolymers.

Experimental section

Materials and characterization

The detailed description about materials and measurements are shown in Section S1 in ESI.† And the detailed process about OLEDs fabrication and testing are also displayed in Section S2 in ESI.†

Syntheses. Spiro[3.3]heptane-2,6-di-(2′,2″,7′,7″-tetrabromospiro fluorene) (**TBrSDF**),[18,20] 3,6-dibromo-*N*-(2-ethylhexyl)-carbazole (**DBrCz**)[21,22] and (Ir(Brpiq)$_2$acac) were synthesized according to the published literature.

General procedure for the synthesis of copolymers

PFCzSDF10Ir6–PFCzSDF10Ir9. To a solution of predetermi ned amount of the monomers (**DBrCz**, 9,9-dioctylfluorene-2,7-bis(trimethyleneboronate) (**M2**), **TBrSDF** and Ir(Brpiq)$_2$acac) in toluene (20 mL) was added an aqueous solution (5 mL) of potassium carbonate (2 M) and a catalytic amount of Pd(PPh$_3$)$_4$ (2.0 mol%). Aliquat 336 (1 mL) in toluene (5 mL) was added as the phase transfer catalyst. The mixture was vigorously stirred at 90 °C for 3 days. Phenylboronic acid was then added to the reaction mixture, followed by stirring at 90 °C for an additional 12 h. Finally, bromobenzene was added in the same way by heating for 12 h again. When cooled to room temperature, the reaction mixture was washed with 2 M HCl and water. The organic layer was separated, and the solution was added dropwise to excess methanol. The precipitates were collected by filtration, and dried under vacuum. The solid was Soxhlet extracted with acetone for 72 h and then passed through a short chromatographic column using toluene as the eluent to afford the copolymers.

PFCzSDF10Ir6. DBrCz (0.153 g, 0.35 mmol), **M2** (0.354 g, 0.55 mmol), **TBrSDF** (0.071 g, 0.1 mmol) and Ir(Brpiq)$_2$acac (0.25 mL, 2 $\times 10^{-3}$ mol L^{-1}). Yield: 75.3%. ^{1}H NMR (CDCl$_3$) δ (ppm): 7.88–7.57 (–ArH–), 6.93–6.89 (–ArH–), 3.41–2.93 (–CH$_2$–),2.21–1.89 (–C–CH$_2$–), 1.18–0.96 (–CH$_2$–), 0.93–0.55 (–CH$_3$).

PFCzSDF10Ir7. DBrCz (0.153 g, 0.35 mmol), **M2** (0.354 g, 0.55 mmol), **TBrSDF** (0.071 g, 0.1 mmol) and Ir(Brpiq)$_2$acac (0.28 mL, 2 $\times 10^{-3}$ mol L^{-1}). Yield: 68.4%. ^{1}H NMR (CDCl$_3$) δ (ppm): 7.89–7.56 (–ArH–), 6.93–6.81 (–ArH–), 3.42–2.93 (–CH$_2$–), 2.21–1.88 (–C–CH$_2$–), 1.19–0.98 (–CH$_2$–), 0.94–0.60 (–CH$_3$).

PFCzSDF10Ir8. DBrCz (0.153 g, 0.35 mmol), **M2** (0.354 g, 0.55 mmol), **TBrSDF** (0.071 g, 0.1 mmol) and Ir(Brpiq)$_2$acac (0.40 mL, 2 $\times 10^{-3}$ mol L^{-1}). Yield: 72.7%. ^{1}H NMR (CDCl$_3$) δ (ppm): 8.06–7.42 (–ArH–), 6.94–6.77 (–ArH–), 3.45–3.02 (–CH$_2$–), 2.24–1.87 (–C–CH$_2$–), 1.19–0.95 (–CH$_2$–), 0.94–0.64 (–CH$_3$).

PFCzSDF10Ir9. DBrCz (0.153 g, 0.35 mmol), **M2** (0.354 g, 0.55 mmol), **TBrSDF** (0.071 g, 0.1 mmol) and Ir(Brpiq)$_2$acac (0.45 mL, 2 $\times 10^{-3}$ mol L^{-1}). Yield: 71.5%. ^{1}H NMR (CDCl$_3$) δ (ppm): 7.98–7.48 (–ArH–), 6.93–6.78 (–ArH–), 3.39–3.02 (–CH$_2$–), 2.21–1.75 (–C–CH$_2$–), 1.22–0.88 (–CH$_2$–), 0.86–0.45 (–CH$_3$).

Table 1 Polymerization and characterizations results of the polymers

						GPC	
Copolymers	n_{DBrCz}	n_{M2}	n_{TBrSDF}	n_{red}	Yield (%)	M_n	PDI
PFCzSDF10Ir6	0.35	0.55	0.10	6×10^{-4}	75.3	9234	1.94
PFCzSDF10Ir7	0.35	0.55	0.10	7×10^{-4}	68.4	11 193	3.67
PFCzSDF10Ir8	0.35	0.55	0.10	8×10^{-4}	72.7	9936	3.77
PFCzSDF10Ir9	0.35	0.55	0.10	9×10^{-4}	71.5	9588	1.29

Results and discussion

Synthesis and characterization

As shown in Scheme 1, a series of hyperbranched copolymers based on *N*-alkyl and 9-C-alkyl substituted 3,6-carbazole-*co*-2,7-fluorene branches with SDF (10 mol%) as the branch point were synthesized by one-pot Suzuki polycondensation in relatively high yields. To obtain efficiently white-light emission, the phosphor red light-emitting unit of Ir(Brpiq)$_2$acac was incorporated into the main chain with the feed ratios of 0.06 mol%, 0.07 mol%, 0.08 mol% and 0.09 mol%, and the corresponding copolymers are named as **PFCzSDF10Ir6**, **PFCzSDF10Ir7**, **PFCzSDF10Ir8** and **PFCzSDF10Ir9**, respectively. The synthetic and structural results of **PPFCzSDF10Ir6–PFCzSDF10Ir9** are summarized in Table 1.

The functional groups for Suzuki polycondensation were bromine and pinacol borate. Thus, the fluorene and carbazole monomers distributed alternately in the synthesized polymer branches. Because of the same feed ratios of monomers **DBrCz**, **M2** and **TBrSDF** for copolymers **PFCzSDF10Ir6–PFCzSDF10Ir9**, their ^{1}H NMR spectra were quite similar (Fig. S4 in ESI†). The proton signals of **Ir(piq)$_2$acac** have little effect because of its low content, revealing the similar backbone structures of the copolymers. The number-average molecular weights (M_n) of the copolymers determined by gel permeation chromatography (GPC) ranged from 9234 to 11 193 with a polydispersity index (PDI) from 1.94 to 3.77. The resulting copolymers are readily soluble in common organic solvents such as trichloromethane ($CHCl_3$), tetrahydrofuran (THF) and toluene.

Thermal properties

The thermogravimetric analysis (TGA) and (differential scanning calorimetry) DSC data of the hyperbranched polymers are shown in Fig. 1 and Table 2. The onset decomposition temperatures (T_d, measured at a 5% weight loss) range from 300 to 416 °C under nitrogen. The high thermal stability is ascribed to the presence of a large amount of carbazole groups and three dimensional structure of the hyperbranched polymers, which are known to exhibit excellent thermal and chemical

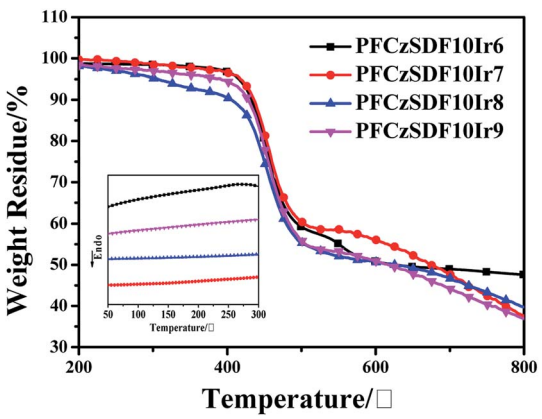

Fig. 1 TGA and DSC (inset) curves of the copolymers in nitrogen atmosphere with a heating rate of 10 °C min^{-1} and 5 °C min^{-1}, respectively.

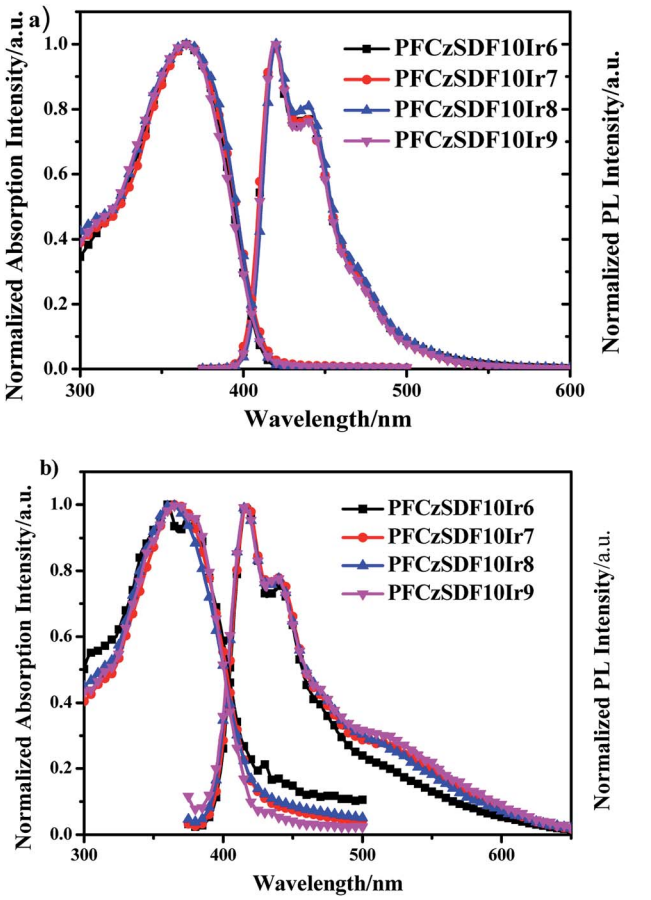

Fig. 2 The UV-vis absorption and PL spectra of the hyperbranched polymers: (a) in $CHCl_3$ solution (10^{-5} M) and (b) in solid film.

Table 2 Thermal and photophysical properties of the copolymers

			Dilute solution		Solid film	
Copolymers	T_d (°C)	T_g (°C)	λ_{abs} (nm)	λ_{PL} (nm)	λ_{abs} (nm)	λ_{PL} (nm)
PFCzSDF10Ir6	413	144	365	419, 438	359 377	417, 440, 520
PFCzSDF10Ir7	420	150	365	419, 438	366	416, 440, 516
PFCzSDF10Ir8	304	175	365	419, 438	362	416, 439, 515
PFCzSDF10Ir9	391	149	364	419, 439	366	416, 438, 519

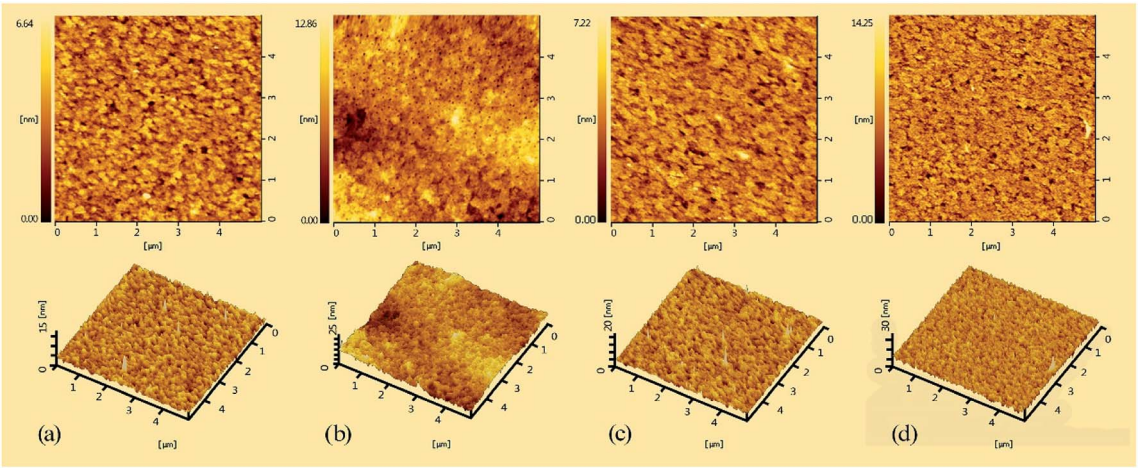

Fig. 3 AFM images (5 × 5 μm) of the copolymer films: (a) for **PFCzSDF10Ir6**, (b) for **PFCzSDF10Ir7**, (c) for **PFCzSDF10Ir8**, and (d) for **PFCzSDF10Ir9**.

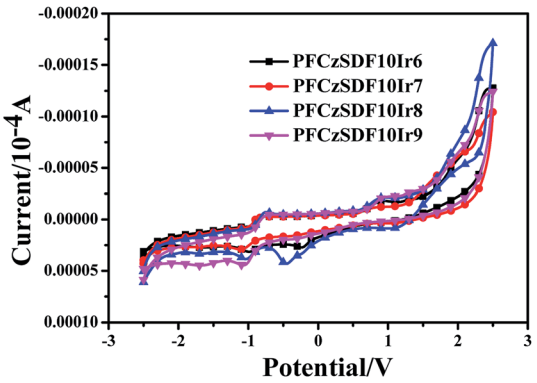

Fig. 4 Cyclic voltammograms curves of the hyperbranched polymers.

stabilities.[23] The relatively high glass transition temperatures (T_g, in inset of Fig. 1) of around 150 °C are found from the DSC curves, which indicates the good morphological stabilities of the copolymers. The high T_g could be attributed to their rigid hyperbranched structures and the introduction of carbazole unit to the copolymer backbones.

Photophysical properties

The UV-vis absorption of **Ir(piq)$_2$acac** and the PL spectra of fluorene-*alt*-carbazole copolymer (PFCz) are shown in Fig. S5.† The absorption of **Ir(piq)$_2$acac** and the emission of PFCz show good spectral overlap, indicating the efficient FRET from the PFCz segment to **Ir(piq)$_2$acac** unit can be expected. The normalized UV-

Table 3 Electrochemical properties of the hyperbranched polymers

Copolymers	$\lambda_{abs(onset)}$ (nm)	E_g (eV)	$E_{onset/ox}$ (V)	HOMO (eV)	LUMO (eV)
PFCzSDF10Ir6	404	3.07	0.93	−5.43	−2.36
PFCzSDF10Ir7	405	3.06	0.86	−5.36	−2.30
PFCzSDF10Ir8	406	3.05	0.90	−5.40	−2.35
PFCzSDF10Ir9	405	3.06	0.94	−5.44	−2.38

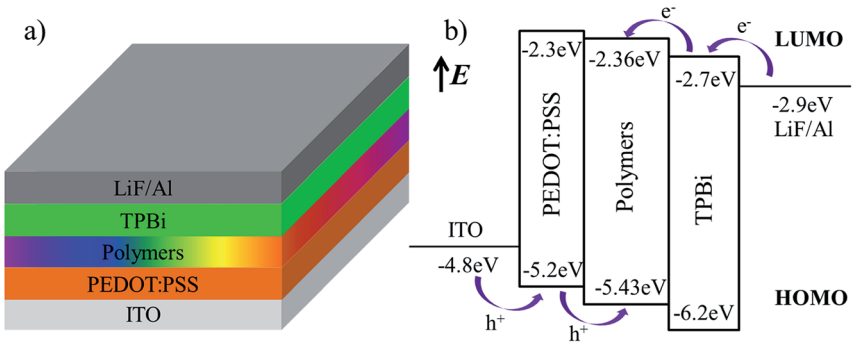

Fig. 5 The device structure (a) and energy-level (b) diagrams of the devices.

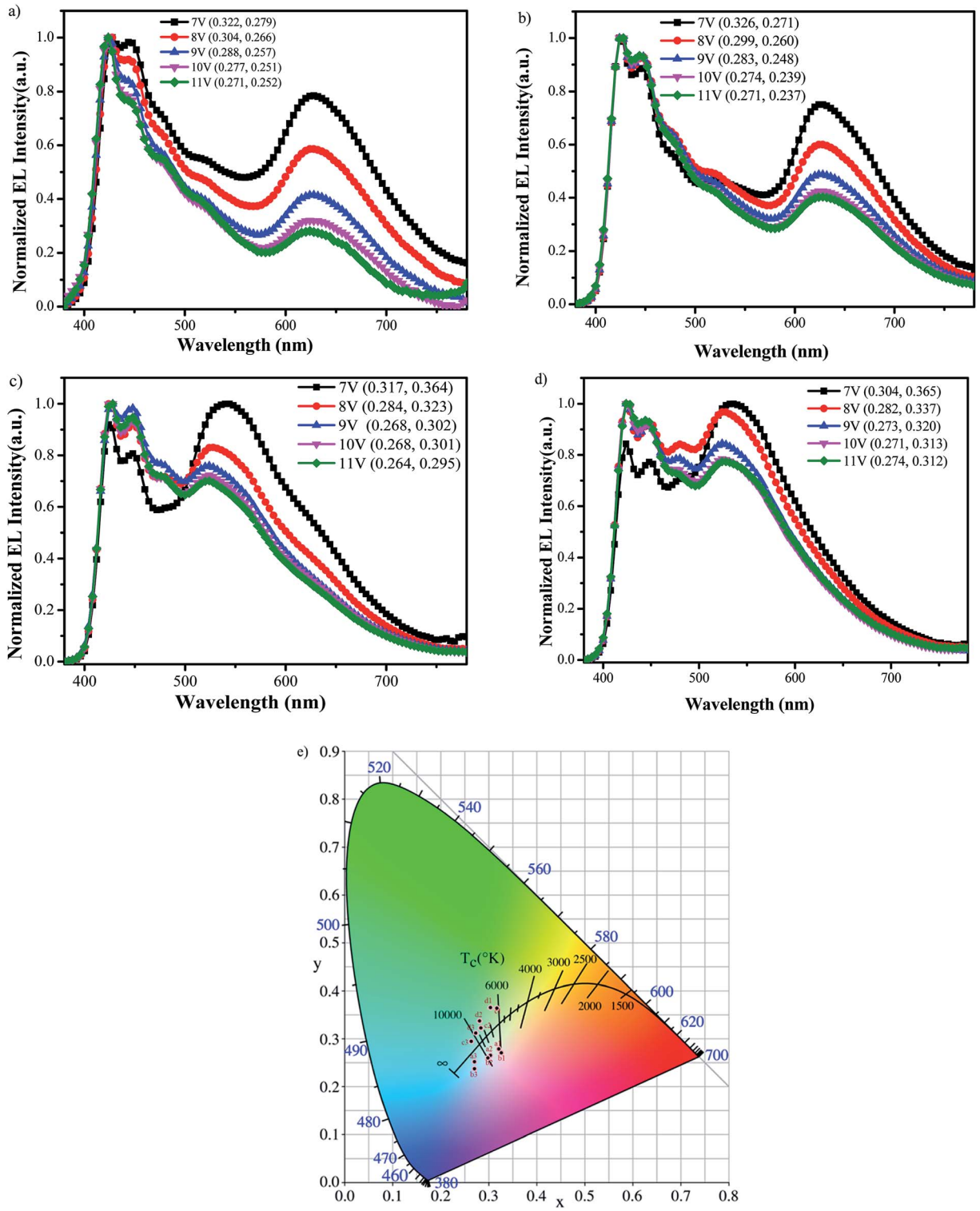

Fig. 6 Electroluminescence spectra of the hyperbranched polymer at different voltages **PFCzSDF10Ir6** (a), **PFCzSDF10Ir7** (b), **PFCzSDF10Ir8** (c) and **PFCzSDF10Ir9** (d) and CIE graph of all polymers at voltages for 7 V, 8 V, and 11 V (e).

vis absorption and photoluminescence (PL) spectra of the copolymers in dilute solution are shown in Fig. 2. The absorption bands at around 365 nm are due to the π–π* transitions of poly(fluorene-*alt*-carbazole) backbones,[24] which are blue-shifted about 15 nm compared with the fluorene-based hyperbranched polymer with SDF of 10 mol%. This notable hypochromatic shift is attributable to the interruption of the conjugation of the copolymer backbone by the introduction of the 3,6-carbazole

linkage. In PL spectra, the copolymers exhibit emission bands at 420 nm and a slight vibronic shoulder at 440 nm, which can be attributed to 0–0 and 0–1 intrachain singlet transitions in the poly(fluorene-*alt*-carbazole) branches.[25] The PL spectra showed about 5 nm blue-shift respect to that of the fluorene-based copolymer because of the decreased conjugated length in these fluorene-*alt*-carbazole based copolymers.

A phosphorescent red group **Ir(piq)$_2$acac** with high internal quantum efficiency as a adjusting group to be introduced into the hyperbranched polymer chain, no distinct absorption or emission peaks of **Ir(piq)$_2$acac** unit can be observed in the spectra because of its relatively lower content in the polymers, and the Förster resonance energy transfer (FRET) is exclusively intrachain in dilute solution.[26]

In films, the hyperbranched polymers exhibit UV-vis absorption bands at around 365 nm owing to the π–π* transitions of the poly-(fluorene-*alt*-carbazole) backbones (Fig. 2b and Table 2). In PL spectra, the maximum emission bands of copolymers are at about 416 nm, along with a shoulder at around 439 nm, showing no obvious bathochromic shift with respect to those in dilute solution, indicating that the hyperbranched structure can effectively avoid the red shift caused by intermolecular aggregation.[25,27,28]

Film morphology

The morphology of copolymers films, which is a key factor for PLEDs fabrication, was investigated by atomic force microscopy (AFM) at a tapping mode. Fig. 3 shows the AFM images of **PPFCzSDF10Ir6–PFCzSDF10Ir9** films prepared by spin-coating chlorobenzene solutions of the copolymers (10^{-5} M) on the full ITO glass. The root-mean-square (RMS) roughness values of hyperbranched polymers are 0.96 nm, 1.91 nm, 1.00 nm, and 2.06 nm, respectively. All the films show flat and smooth surface without any pinhole defects. The results imply that the three-dimensional structured SDF branch point can help to form homogeneous films with good quality.[29] The uniform amorphous morphology is favorable for PLEDs fabrication.

Electrochemical characteristics

The electrochemical behaviors of the resulting hyperbranched polymers were investigated by cyclic voltammetry (CV), as shown in Fig. 4 and Table 3. The oxidation potentials (E_{ox}) vary slightly from 0.86 to 0.93 V. The HOMO levels of polymers are calculated according to the empirical formulas $E_{HOMO} = -(E_{ox} + 4.5)$ (eV),[5] they are at about −5.40 eV. The lowest unoccupied molecular orbital (LUMO) levels are deduced from the HOMO levels and the optical band gaps (E_g) determined from the onset value of the absorption spectrum in film in the long-wavelength direction ($E_g = 1240/\lambda_{edge}$), and they are at −2.30 eV to −2.38 eV. The HOMO levels of the hyperbranched polymers are slightly deeper than the work function (−5.2 eV) of PEDOT:PSS, which imply the facile hole injection from PEDOT:PSS to hyperbranched polymers emission layer (EML) can be expected.[30] On the other hand, the LUMO levels of the hyperbranched polymers are slightly shallower than that (−2.7 eV) of electron transporting 1,3,5-tri(1-phenyl-1*H*-benzo[*d*]imidazol-2-yl)phenyl (TPBi), indicating that the barrier for electron injection is relatively small from electron transporting layer to hyperbranched polymer EML.

Electroluminescent properties

Based on good photoelectric performance and suitable energy level for above hyperbranched polymers, we further evaluate the their EL performance by fabricating the PLEDs with the configuration of ITO/PEDOT:PSS (40 nm)/polymers (50 nm)/TPBi (45 nm)/LiF (1 nm)/Al (150 nm). The device structure and energy-level diagrams of all devices are shown in Fig. 5a and b, respectively. In these devise, ITO and Al are used as anode and cathode, respectively; PEDOT:PSS and TPBi are used as hole transport layer and electron transport layer, respectively; 50 nm-thick polymers layer is used as EML, and 1 nm-thick LiF layer used as electron injection layer.[1,31–35]

Fig. 6a–d shows the EL spectra for all polymers-based PLEDs at voltages varying from 7 to 11 V. It can be seen that all resulting PLEDs with **PFCzSDF10Ir6**, **PFCzSDF10Ir7**, **PFCzSDF10Ir8**, **PFCzSDF10Ir9** as realize good white emission with CIE coordinate of at (0.27,0.25), (0.27,0.24), (0.26,0.30), and (0.27,0.31) at 11 V, respectively, and the EL spectra for these PLEDs all contain two main emission peaks located at blue and orange-red wavebands, which are corresponding to the emissions of poly(fluorene-*alt*-carbazole) branches and red dimming phosphor group (**Ir(piq)$_2$acac**). This is ascribed to the incomplete Förster energy transfer in intra-, and interchain interaction of polymer layer from **PFCz** segment to **Ir(piq)$_2$acac** unit. With the Ir(Brpiq)$_2$acac feed ratios from 0.06 mol%, 0.07 mol%, 0.08 mol% to 0.09 mol% in synthesis processes, corresponding to **PFCzSDF10Ir6**, **PFCzSDF10Ir7**, **PFCzSDF10Ir8** and **PFCzSDF10Ir9**, respectively, the orange-red wavebands from (**Ir(piq)$_2$acac**) in EL spectra present an increasing trend, indicating the EL spectra of polymers-based PLEDs can be realized and adjusted by simply changing the Ir(Brpiq)$_2$acac feed ratios in synthesis processes. For individual PLED, we can see that under low voltage, the longer wavelength orange-red emission in EL spectra is the strongest, and with the increase of drive voltage from 7 V to 11 V, the longer wavelength orange-red emission reduced gradually, and keep almost overlapping EL spectra at 10–11 V for all PLEDs. This is because the exciton energy can easily transfer to lower energy level of **Ir(piq)$_2$acac**, leading to stronger orange-red emission form **Ir(piq)$_2$acac**,

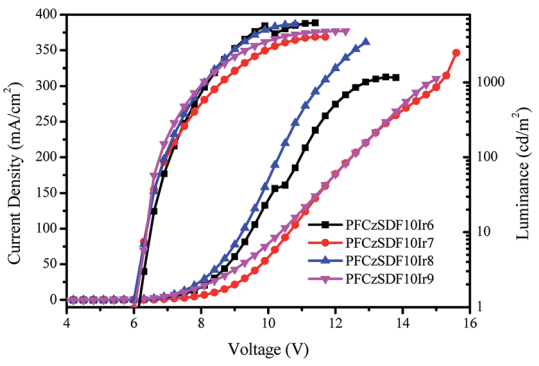

Fig. 7 Current density–voltage–brightness (*J*–*V*–*L*) curves characteristics of hyperbranched polymers light emitting devices.

Table 4 EL Performances of the PLEDs

Copolymer	V_{on}[a](V)	L_{max}[b](cd m^{-2}) (at the voltage (V))	CE_{max} (cd A^{-1})	LE_{max} (lm W^{-1})	CIE[c](x,y)	CRI[c]	CCT[c]
PFCzSDF10Ir6	6.00	5946	3.57	1.31	(0.27,0.25)	67	11 432
PFCzSDF10Ir7	6.10	4827.7	5.23	1.95	(0.27,0.24)	70	19 427
PFCzSDF10Ir8	6.10	6210	4.65	1.65	(0.26,0.30)	90	9387
PFCzSDF10Ir9	6.10	4024.5	6.30	2.68	(0.27,0.31)	88	8999

[a] Turn-on voltage (at 1 cd m^{-2}). [b] Maximum luminance at applied voltage. [c] CIE, CRI and CCT values measured at a voltage of 11 V for devices a–d.

but with the increase of drive voltage, the site of **Ir(piq)$_2$acac** can be easily saturated, inducing a reduced orange-red emission in EL spectra. The difference in the PL and EL spectra imply that different mechanisms should be involved. In photoluminescence excitation (PLE), the PFCz moiety is in a single excited state and the energy is transferred to the Ir(III) complex. In electroluminescent excitation, electrons are injected from the cathode in the device, and holes are injected from the anode and then trapped by the Ir(III) complex. The results reveal that the intra-, interchain FRET from PFCz unit to **Ir(piq)$_2$acac** and the charge trapping of **Ir(piq)$_2$acac** happen simultaneously in the electroluminescence process.

Fig. 7 shows the current density–voltage–luminance (*J–V–L*) characteristics curves of all hyperbranched polymers-based devices, and the basic electroluminescence properties of the device are summarized in Table 4. It can be seen that the maximum luminance (~6210 cd m^{-2}) for **PFCzSDF10Ir8**-based device and the maximum current efficiency (~6.30 cd A^{-1}) of **PFCzSDF10Ir9**-based device are obtained. Further investigations on the optimization of the device performance and the synthesis of hyperbranched polymers with different structure and color groups are ongoing in our laboratory.

Conclusions

In this work, a series of hyperbranched copolymers with fluorene-*alt*-carbazole as the branches, three-dimensional-structured spiro [3.3]heptane-2,6-dispirofluorene (SDF) as the core, and iridium 1-(4-bromophenyl)-isoquinoline (acetylacetone) (Ir(Brpiq)$_2$acac) as dimming group were synthesized by one-pot Suzuki polycondensation for white emission. All synthesized hyperbranched polymers show a three-dimensional structure with very good morphological stability and strong fluorescence characteristics. And such three-dimensional structure can also effectively inhibit the entanglement of adjacent alkyl chains through its large steric hindrance, reducing the tight packing of molecular chains and the interaction between the various chromophores in the solid state. The fabricated polymer light-emitting devices (PLEDs) based above synthesized copolymers realize good white light emission, and achieve high electroluminescence (EL) performance. For example, for the optimized PLED, the maximum luminance and current efficiency reach 6210 cd m^{-2} and 6.30 cd A^{-1}, respectively. These results indicate that the hyperbranched polymers using SDF as the core and fluorene-*alt*-carbazole as the branches and phosphorescent adjusting group could be promising candidates as white-emitting materials with high efficiency.

Conflicts of interest

The authors declare no competing financial interest.

Acknowledgements

The authors are grateful to the "the National Natural Science Foundation of China (61705158, 61605138, 61605137, 61775155, 61705156), Shanxi Province Natural Science Foundation (201601D202030, 201601D021018, 201601D011031, 201801D221102); and Scientific and Technological Innovation Programs of Higher Education Institutions in Shanxi (2019L0302, 2016134, 2016135, 201802111).

Notes and references

1 T. Guo, R. Guan, J. Zou, J. Liu, L. Ying, W. Yang, H. Wu and Y. Cao, *Polym. Chem.*, 2011, **2**, 2193.
2 T. Guo, L. Yu, Y. Yang, Y. Li, Y. Tao, Q. Hou, L. Ying, W. Yang, H. Wu and Y. Cao, *J. Lumin.*, 2015, **167**, 179–185.
3 S. H. Hwang, C. D. Shreiner, C. N. Moorefield and G. R. Newkome, *New J. Chem.*, 2007, **31**, 1192.
4 F. Liu, J. Q. Liu, R.-R. Liu, X.-Y. Hou, L.-H. Xie, H.-B. Wu, C. Tang, W. Wei, Y. Cao and W. Huang, *J. Polym. Sci., Part A: Polym. Chem.*, 2009, **47**, 6451–6462.
5 Y. Wu, J. Li, W. Liang, J. Yang, J. Sun, H. Wang, X. Liu, B. Xu and W. Huang, *RSC Adv.*, 2015, **5**, 49662–49670.
6 J. Sun, J. Yang, C. Zhang, H. Wang, J. Li, S. Su, H. Xu, T. Zhang, Y. Wu, W.-Y. Wong and B. Xu, *New J. Chem.*, 2015, **39**, 5180–5188.
7 L. R. Tsai and Y. Chen, *J. Polym. Sci., Part A: Polym. Chem.*, 2007, **45**, 4465–4476.
8 A. Pfaff and A. H. E. Müller, *Macromolecules*, 2011, **44**, 1266–1272.
9 B. Bao, L. Yuwen, X. Zhan and L. Wang, *J. Polym. Sci., Part A: Polym. Chem.*, 2010, **48**, 3431–3439.
10 L. R. Tsai and Y. Chen, *Macromolecules*, 2008, **41**, 5098–5106.
11 D. Konkolewicz, C. K. Poon, A. Gray-Weale and S. Perrier, *Chem. Commun.*, 2011, **47**, 239–241.
12 J. Liu, Y. Cheng, Z. Xie, Y. Geng, L. Wang, X. Jing and F. Wang, *Adv. Mater.*, 2008, **20**, 1357–1362.
13 L. Ying, C. L. Ho, H. Wu, Y. Cao and W. Y. Wong, *Adv. Mater.*, 2014, **26**, 2459–2473.
14 S. J. Su and X. L. Li, *White Organic Light-Emitting Diodes*, 2016.

15 X. H. Zhu, J. Peng, Y. Cao and J. Roncali, *Chem. Soc. Rev.*, 2011, **40**, 3509–3524.
16 B. Zhang, G. Tan, C. S. Lam, B. Yao, C. L. Ho, L. Liu, Z. Xie, W. Y. Wong, J. Ding and L. Wang, *Adv. Mater.*, 2012, **24**, 1873–1877.
17 Y. Miao, X. Wei, L. Gao, K. Wang, B. Zhao, Z. Wang, B. Zhao, H. Wang, Y. Wu and B. Xu, *Nanophotonics*, 2019, **8**, 1783–1794.
18 Z. Wang, L. Zheng, J. Wang and W. Du, *Complexity*, 2019, 4031795.
19 W. Y. Wong, *Coord. Chem. Rev.*, 2005, **249**, 971–997.
20 Z. Wang, J. Wang, W. Cai, J. Zhou, W. Du, J. Wang, G. He and H. He, *Complexity*, 2019, 1564243.
21 J. Kim, S. H. Park, S. Cho, Y. Jin, J. Kim, I. Kim, J. S. Lee, J. H. Kim, H. Y. Woo, K. Lee and H. Suh, *Polymer*, 2010, **51**, 390–396.
22 H. Wang, J. T. Ryu and Y. Kwon, *J. Appl. Polym. Sci.*, 2011, **119**, 377–386.
23 T. Sudyoadsuk, P. Moonsin, N. Prachumrak, S. Namuangruk, S. Jungsuttiwong, T. Keawin and V. Promarak, *Polym. Chem.*, 2014, **5**, 3982.
24 J. Li, R. Liu, Z. Zhao and Z. Zhou, *J. Mater. Sci.: Mater. Electron.*, 2014, **25**, 1970–1975.
25 J. Yang, C. Jiang, Y. Zhang, R. Yang and Y. Y. Cao, *Macromolecules*, 2004, **37**, 1211–1218.
26 L. Ying, Y. Xu, W. Yang, L. Wang, H. Wu and Y. Cao, *Org. Electron.*, 2009, **10**, 42–47.
27 Z. Wang, P. Lu, S. Xue, C. Gu, Y. Lv, Q. Zhu, H. Wang and Y. Ma, *Dyes Pigm.*, 2011, **91**, 356–363.
28 W. Hua, X. U. Yang, T. Tsuboi, X. U. Huixia, W. U. Yuling, Z. Zhang, Y. Miao, Y. Hao and X. Liu, *Org. Electron.*, 2013, **14**, 827–838.
29 Y. Wu, J. Li, W. Liang, J. Yang, J. Sun, H. Wang, X. Liu, B. Xu and W. Huang, *New J. Chem.*, 2015, **39**, 5977–5983.
30 M. Zhu, Y. Li, J. Miao, B. Jiang, C. Yang, H. Wu, J. Qin and Y. Cao, *Org. Electron.*, 2014, **15**, 1598–1606.
31 Y. Miao, K. Wang, B. Zhao, L. Gao, P. Tao, X. Liu, Y. Hao, H. Wang, B. Xu and F. Zhu, *Nanophotonics*, 2018, **7**, 295–304.
32 Y. Miao, P. Tao, K. Wang, H. Li, B. Zhao, L. Gao, H. Wang, B. Xu and Q. Zhao, *ACS Appl. Mater. Interfaces*, 2017, **9**, 37873–37882.
33 Y. Miao, K. Wang, L. Gao, B. Zhao, H. Wang, F. Zhu, B. Xu and D. Ma, *J. Mater. Chem. C*, 2018, **6**, 8122–8134.
34 P. Tao, Y. Miao, H. Wang, B. Xu and Q. Zhao, *Chem. Rec.*, 2019, **19**, 1531–1561.
35 Y. Wu, X. Li, H. Zhao, J. Li, Y. Miao, H. Wang, F. Zhu and B. Xu, *Org. Electron.*, 2020, **76**, 105487.